



Published in final edited form as:

*Otolaryngol Head Neck Surg.* 2017 September ; 157(3): 448–453. doi:10.1177/0194599817700388.

## Coherent Raman Scattering Microscopy for Evaluation of Head and Neck Carcinoma

Rebecca C. Hoesli, MD<sup>1</sup>, Daniel A. Orringer, MD<sup>2</sup>, Jonathan B. McHugh, MD<sup>1</sup>, and Matthew E. Spector, MD<sup>1</sup>

<sup>1</sup>Department of Otolaryngology-Head and Neck Surgery, University of Michigan Health System, Ann Arbor, Michigan

<sup>2</sup>Department of Neurosurgery, University of Michigan Health System, Ann Arbor, Michigan

### Abstract

**Objective**—We aim to describe a novel, label-free, real-time imaging technique, coherent Raman scattering (CRS) microscopy, for histopathological evaluation of head and neck cancer. We evaluated the ability of CRS microscopy to delineate between tumor and non-neoplastic tissue in tissue samples from head and neck cancer patients.

**Study Design**—Prospective Case Series

**Setting**—Tertiary Care Medical Center

**Subjects and Methods**—Patients eligible were surgical candidates with biopsy proven, previously untreated head and neck carcinoma and were consented pre-operatively for participation in this study. Tissue was collected from 50 patients, and after confirmation of tumor and normal specimens by H&E, there were 42 tumor samples and 42 normal adjacent controls.

**Results**—There were 42 confirmed carcinoma specimens on H&E, CRS microscopy identified 38 as carcinoma. Of the 42 normal specimens, CRS microscopy identified 40 as normal. This resulted in a sensitivity of 90.5% and specificity of 95.2% in distinguishing between neoplastic and non-neoplastic images.

**Conclusion**—CRS microscopy is a unique label free imaging technique that can provide rapid, high-resolution images, and can accurately determine the presence of head and neck carcinoma. This holds potential for implementation into standard practice, allowing frozen margin evaluation even at institutions without a histopathology laboratory.

### Introduction

Despite advances in the diagnosis and treatment of head and neck carcinoma, it remains a formidable source of morbidity and mortality. In North America alone, more than 50,000 new cases of head and neck cancer are diagnosed yearly, and more than 12,000 deaths were estimated to occur due to head and neck cancer in 2015<sup>1</sup>. The majority of these cancers are

---

Corresponding Author: Matthew E. Spector, M.D., 1500 E. Medical Center Dr., 1904 Taubman Health Center, SPC 5312, Ann Arbor, MI 48109-5312, (734)936-3172 Phone, (734)936-9625 Fax, mspector@med.umich.edu.

This study was presented at the 2016 AAO-HNSF Annual Meeting

related to head and neck squamous cell carcinoma of the upper aerodigestive mucosa<sup>1</sup>. Tobacco and alcohol use are the main risk factors associated with the development of head and neck cancer, but the incidence of oropharyngeal cancer related to Human Papilloma Virus (HPV) has been rising<sup>2</sup>. Due to its continued prevalence, morbidity, and mortality, head and neck carcinoma remains a major health problem in the world today.

Surgical intervention is a cornerstone of treatment for many head and neck cancers. In surgically treated head and neck cancer, margin status is one of the most important prognostic factors, with a positive surgical margin correlating with higher rates of local recurrence and lower rates of survival<sup>3</sup>. Unfortunately, in the head and neck, margins can be difficult to map and interpret due to the complex three-dimensional anatomy of the head and neck and close proximity of critical structures that cannot be resected<sup>3</sup>.

While intraoperative frozen sections using Hematoxylin and Eosin (H&E) staining is widely accepted, there are downsides of this technique. Limitations include sampling errors between the margin, specimen and resection bed, with discordance between whether or not to resect more “normal tissue” posing a difficult problem to the surgeon.<sup>4,5</sup> Additionally, studies on the frozen section analysis in head and neck carcinoma reveal the sensitivity to be between 83.1-88.8%, allowing for a false negative rate which can result in unrecognized residual disease<sup>4-6</sup>. Finally, frozen section analysis is time and resource consuming. It requires a functioning histopathology lab and extends the length of time the patient is under anesthesia while an experienced, in-facility histopathologist processes, stains, and evaluates the specimen.

Coherent Raman scattering (CRS) microscopy, which includes coherent anti-stokes Raman scattering (CARS) microscopy and stimulated Raman scattering (SRS) microscopy, is a unique label-free imaging technique that overcomes many of the limitations of standard microscopic methods. The CRS microscope analyzes the molecular composition of a sample by using the intrinsic vibrational characteristics of the various molecules including lipids, proteins, and DNA to provide contrast for the images<sup>7</sup>. The vibrational characteristics of CH<sub>2</sub> highlights lipid-rich structures, while the vibrational characteristics of CH<sub>3</sub> molecules highlights the protein and DNA rich structures, like nuclei, to create a virtual image<sup>8</sup>. Because CRS microscopy uses the intrinsic characteristics of these molecules, no processing, staining, or labeling is required, thereby increasing the efficiency of specimen evaluation.

CRS microscopy can also optically section specimens, and thus can be used to evaluate even thick specimens, improving the ease of evaluating three-dimensional surgical margins. Due to the nature of the microscope, specimens can be imaged at up to 30 frames per second producing real-time microscopic tissue imaging that improves the rate of specimen evaluation<sup>9</sup>. This increased efficiency allows for streamlined specimen processing and could allow for improved accuracy in the delineation of tumor extent. Finally, because the images are digital, they can easily be stored, quality-controlled, and incorporated into infrastructure research databases and electronic medical records. Additionally, should a facility not be equipped with a histopathology lab, images could be sent off site for real-time evaluation by a histopathologist.

CRS microscopy has been previously validated for use in neurosurgery for delineating tumor from non-neoplastic tissue. In these studies, CRS has excellent agreement with standard H&E imaging in assessing tumor infiltration<sup>10,11</sup>. CRS microscopy has not previously been evaluated for use in identifying margin status in head and neck cancer or for use in diagnosing head and neck carcinomas. As a result, we evaluated the ability of CRS microscopy to delineate between tumor and non-neoplastic tissue in tissue samples from head and neck cancer patients.

## Methods

Eligible patients were surgical candidates with biopsy proven, previously untreated head and neck carcinoma. Patients were consented pre-operatively for participation in this study, which was approved by the University of Michigan IRB (HUM00095967 and HUM00042189). Tissue was obtained from 50 patients. Frozen margins were sent as the standard of care and surgery. Additional margins were taken based on the results of the H&E frozen margins only.

Tumor biopsies and the normal controls were placed on slides, and no further processing, staining, or labeling was performed. We then used a two-color stimulated Raman scattering microscopy method for imaging the human head and neck tumors. This microscope has previously been described in neurosurgical patients<sup>8</sup>. In brief, the microscope consists of a tunable pump beam (650 to 1000nm) which is combined with a Stokes beam (1064nm) from a fiber laser module tuned through the laser control module. The specimen was placed on the microscope stage of a fiber coupled microscope, and these beams are then focused on to the sample. The sample causes an intensity loss in the pump beam which correlates to the ratio of lipid and protein found in the sample. This intensity loss between the two beams is detected, and the variation in the lipid/protein ratio provides the contrast in the microscopic images which is displayed on a computer (Figure 1).

Two separate scans are performed per field of view. For these scans, the Stokes beam is fixed at 1064nm and the other the beam is focused at either  $2845\text{ cm}^{-1}$ , which highlights the characteristics of the  $\text{CH}_2$  stretching vibrations, or  $2940\text{ cm}^{-1}$  which highlights the characteristics of the  $\text{CH}_3$  stretching vibrations.  $\text{CH}_2$  primarily highlights lipids in the cytoplasm, while the  $\text{CH}_3$  image highlights lipids and proteins. The microscope scanning software acquires each image and then processes it via ImageJ (v1.49) (Figure 2). Multiple consecutive fields of view are then collated and aligned to produce the final image.

To assess the ability of CRS microscopy to delineate between tumor and non-neoplastic tissue when compared to the gold standard of H&E, tumor specimens were removed from the microscope slide after imaging and sent to the University of Michigan histopathology core for processing and H&E staining. The fixed specimens were randomized then read independently as either tumor or normal tissue by a senior head and neck pathologist (JBM). Patients were excluded if there was not gross tumor present in the H&E tumor specimen. There were five tumor samples that were shown by H&E to contain benign scar and normal tissue and three tumor samples that were shown by H&E to contain minimal cancer. Of the 50 patients, there were 42 tumor samples and 42 normal adjacent controls that were

confirmed on H&E. The CRS images were randomized separately and then read by the same pathologist using a separate color lookup table. Results were tabulated and the sensitivity and specificity of CRS was calculated using H&E as the gold standard. Images were classified in a binary fashion as “tumor” or “normal”.

## Results

Tumor characteristics are shown in Table 1. The five two additional samples not confirmed as carcinoma were found to be benign scar and normal tissue.

Of the 42 confirmed carcinoma specimens, CRS microscopy successfully identified 38 as carcinoma. Of the 42 normal specimens, CRS microscopy successfully identified 40 as normal. This resulted in a sensitivity of 90.5% and specificity of 95.2% in distinguishing between neoplastic and non-neoplastic images (Table 2).

In order to understand the discordant cases in this study, we further examined the incorrectly identified specimens. Three of the specimens were imaged in the first month of imaging, likely representing poor imaging quality due to user error while learning the process of CRS microscopy. During this time period, adaptation of CRS microscopy for head and neck tumors was occurring, and thus many of these specimens were not ideally sectioned for imaging with CRS microscopy. We realized that careful orientation and thinner sectioning of tissue produced higher quality images. This would eliminate 6 tumor samples, 3 of which showed discordance with CRS imaging. After development of a tissue handling protocol which involved properly sectioning the specimens, the authors saw an increase in the efficiency and quality of the images produced, along with an increase in the overall sensitivity to 94.4% which is *higher than* previously demonstrated sensitivity of frozen margins<sup>6</sup>.

## Discussion

In head and neck carcinoma, margin status is critically important to adequate treatment, as positive margin status correlates with higher risk of recurrence and decreased survival<sup>3</sup>. However, adequate margins are often difficult to obtain in the head and neck due to the complex anatomy as well as the close proximity of vital structures, such as the carotid artery, which cannot be resected. At this time, frozen margins are the gold standard for determining intraoperative margin status, but this technique still results in false negatives due to discordance between the margin, specimen, and surgical bed, and adds operative time. Additionally, an in-facility histopathology lab with well-trained histopathologists are critical to the accurate diagnosis of intraoperative frozen margins.

Here, we demonstrated in this early report that CRS microscopy can be used to differentiate between neoplastic and non-neoplastic tissue in head and neck carcinoma. CRS microscopy adequately demonstrates the atypical nuclei and hypercellularity characteristically seen in head and neck squamous cell carcinoma as compared with H&E (Figure 3). In head and neck tumors, overall sensitivity was found to be 84.4%, with a specificity of 95.2%. CRS microscopy was found to be easily performed and efficient, with acquisition and creation of the CRS slide taking less than 30 seconds.

CRS microscopy images were digital and thus could be easily transferred to the medical record or uploaded off-site for histopathology evaluation by a tertiary care center, should a histopathologist not be present on-site or should a second opinion be required. Secondary evaluation of surgical pathology has been found in several studies to significantly impact treatment and diagnosis of head and neck cancer patients<sup>12</sup>, and thus CRS microscopy could facilitate increased utilization of second opinions, even in real time, which could improve patient care.

Evaluation of CRS images, similar to H&E, requires training by the histopathologist. Additionally, this study did not have the benefit of real-time margin acquisition, and when a sample that was imaged had poor tissue quality, and thus was likely “non-diagnostic”, additional samples were not able to be obtained as occurs in standard frozen-margin evaluation. With further experience with CRS images and with the benefit of obtaining additional specimens should further tissue be required, we hypothesize that CRS microscopy would continue to demonstrate equal to or improved sensitivity in diagnosing head and neck carcinoma as compared to H&E staining. Additionally, as we have discussed, CRS microscopy has the added benefit of creating digital images which can facilitate second opinions and inter-facility cooperation.

Due to its importance, multiple imaging techniques have been developed to evaluate margin status. Other imaging techniques, including optical coherence tomography<sup>13</sup> and confocal reflection,<sup>14</sup> have been evaluated for use in margin status, but do not delineate non-neoplastic tissue from normal tissue as accurately as CRS microscopy<sup>10</sup>. In head and neck cancer, scattered Raman spectroscopy (SRS) has been evaluated for use in the detection of tumor infiltration in a few studies<sup>15-17</sup>. In one study in particular, scattered Raman spectroscopy was used to evaluate the lipid, connective tissue, and protein content of tissues, and then this was used to differentiate between tumor and normal tissue. This study laid the groundwork for Raman spectroscopy use in head and neck carcinoma as it did show promising results in the differentiation between normal and neoplastic tissue<sup>15</sup>. However, unlike coherent Raman spectroscopy, scattered Raman spectroscopy has long integration times resulting in only point acquisition of images. Additionally, due to the process of scattered Raman spectroscopy, SRS microscopy has poorer image quality that limits its translation into clinical applications. Finally, in cutaneous carcinoma, CRS microscopy has also been evaluated against standard H&E imaging and reflectance confocal microscopy (RCM)<sup>18</sup>. RCM is currently the most widely used non-invasive high-resolution optical imaging technique which has gained clinical acceptance for evaluation of cutaneous carcinomas<sup>18</sup>. When compared with these modalities in diagnosing cutaneous carcinomas, CRS was found to demonstrate the same level of detail and histopathological information as H&E stained images, and provided more detail than observed with RCM<sup>18</sup>. CRS microscopy has thus far shown substantial promise in its ability to be used clinically, and has significant benefits over other imaging techniques.

An important limitation of this technology is the learning curve around tissue processing and using the microscope. Our first six samples required us to modify our technique, that careful orientation and thinner sectioning of tissue produced higher quality images. Studies on the frozen section analysis in head and neck carcinoma reveal the sensitivity to be between

83.1-88.8%, and with our improved processing technique we were able to increase our sensitivity to 84.4%<sup>4-6</sup>.

While this technology is increasingly being used in clinical scenarios<sup>19</sup> there are a number of future studies that must be performed before adding CRS microscopy to the clinical armamentarium. Future studies will require a larger prospective cohort to expand and validate this technology in head and neck cancer margins. Another important consideration will be to examine HPV-related malignancies, field cancerization effects, and dysplastic epithelium to determine the ability of CRS to distinguish between these commonly encountered tissues in head and neck pathology. Additionally, future studies will examine the role of CRS microscopy in the diagnosis of other types of head and neck carcinoma which do not currently have an adequate method of obtaining intraoperative margins, such as melanoma. Finally, a study must be performed to evaluate whether CRS microscopy can be easily performed and interpreted by other fellowship trained head and neck pathologists with similar sensitivity and specificity rates.

## Conclusion

CRS microscopy is a unique, label free imaging technique that produces images demonstrating a similar sensitivity and specificity to routine H&E histopathology in determining carcinoma from benign tissue in this initial study after appropriate tissue processing protocols were developed. It produces digital images that can be easily incorporated into an electronic medical record, and could facilitate second opinions by an experienced histopathologist, thus improving patient care. CRS microscopy has the great potential to improve the efficiency and possibly the accuracy of margin status determination in head and neck cancer.

## References

1. American Cancer Society. Cancer Facts & Figures 2015. Atlanta, GA: American Cancer Society; 2015.
2. Pezzuto F, Buonaguro L, Caponigro F, et al. Update on Head and Neck Cancer: Current Knowledge on Epidemiology, Risk Factors, Molecular Features and Novel Therapies. *Oncology*. 2015; 89:125–136. [PubMed: 25967534]
3. Chen TC, Wang CP, Koa JY, Yang TL, Lou PJ. The impact of pathologic close margin on the survival of patients with early stage oral squamous cell carcinoma. *Oral Oncology*. 2012; 48(7): 623–628. [PubMed: 22349276]
4. Ord RA, Aisner S. Accuracy of frozen sections in assessing margins in oral cancer resection. *J Oral Maxillofac Surg*. 1997; 55(7):662–669.
5. DiNardo LJ, Lin J, Karageorge LS, Powers CN. Accuracy, utility, and cost of frozen section margins in head and neck cancer surgery. *Laryngoscope*. 2000; 110:1773–1776. [PubMed: 11037842]
6. Du E, Ow TJ, Lo YT, et al. Refining the utility and role of Frozen section in head and neck squamous cell carcinoma resection. *Laryngoscope*. 2016; 126(8):1768–1775. [PubMed: 27113207]
7. Freudiger CW, Min W, Saar BG, Lu S, Holtom GR, He C, Tsai JC, Kang JX, Xie XS. Label-free biomedical imaging with high sensitivity by stimulated Raman scattering microscopy. *Science*. 2008; 322:1857–1861. [PubMed: 19095943]
8. Freudiger CW, Pfannl R, Orringer DA, Saar BG, Ji M, Zeng Q, Ottoboni L, Ying W, Waeber C, Sims JR, De Jager PL, Sagher O, Philbert MA, Xu X, Kesari S, Xie XS, Young GS. Multicolored stain-free histopathology with coherent Raman imaging. *Laboratory Investigation*. 2012; 92:1492–1502. [PubMed: 22906986]

9. Saar BG, Freudiger CW, et al. Video-rate molecular imaging in vivo with stimulated Raman scattering. *Science*. 2010; 330:1368. [PubMed: 21127249]
10. Ji M, Orringer DA, Freudiger CW, Ramkissoon S, Liu X, Lau D, Golby AJ, Norton I, Hayashi M, Agar NY, Young GS, Spino C, Santagata S, Camelo-Piragua S, Ligon KL, Sagher O, Xie XS. Rapid, label-free detection of brain tumors with stimulated Raman scattering microscopy. *Sci Transl Med*. 2013 Sep 4.5(201):201ra119.
11. Ji M, Lewis S, Camelo-Piragua S, Ramkissoon SH, Snuderl M, Venneti S, Fisher-Hubbard A, Garrard M, Fu D, Wang AC, Heth JA, Maher CO, Sanai N, Johnson TD, Freudiger CW, Sagher O, Xie XS, Orringer DA. Detection of human brain tumor infiltration with quantitative stimulated Raman scattering microscopy. *Sci Transl Med*. 2015 Oct 14.7(309):309ra163.
12. Westra WH, Kronz JD, Eisele DW. The impact of second opinion surgical pathology on the practice of head and neck surgery: A decade experience at a large referral hospital. *Head & Neck*. 2002; 24(7):684–693. [PubMed: 12112543]
13. Böhringer HJ, Lankenau E, Stellmacher F, Reusche E, Hüttmann G, Giese A. Imaging of human brain tumor tissue by near-infrared laser coherence tomography. *Acta Neurochir (Wien)*. 2009; 151:507–517. [PubMed: 19343270]
14. Georges J, Zehri A, Carlson E, Nichols J, Mooney MA, Martirosyan NL, Ghaffari L, Kalani MY, Eschbacher J, Feuerstein B, Anderson T, Preul MC, Van Keuren-Jensen K, Nakaji P. Label-free microscopic assessment of glioblastoma biopsy specimens prior to biobanking. *Neurosurg Focus*. 2014; 36:E8. [corrected].
15. Cals FL, Bakker Schut TC, Hardillo JA, Baatenburg de Jong RJ, Koljenovic S, Puppels GJ. Investigation of the potential of Raman spectroscopy for oral cancer detection in surgical margins. *Lab Invest*. 2015 Oct; 95(10):1186–96. [PubMed: 26237270]
16. Barroso EM, Smits RW, Bakker Schut TC, ten Hove I, Hardillo JA, Wolvius EB, Baatenburg de Jong RJ, Koljenovi S, Puppels GJ. Discrimination between oral cancer and healthy tissue based on water content determined by Raman spectroscopy. *Anal Chem*. 2015 Feb 17; 87(4):2419–26. [PubMed: 25621527]
17. Guze K, Pawluk HC, Short M, Zeng H, Lorch J, Norris C, Sonis S. Pilot study: Raman spectroscopy in differentiating premalignant and malignant oral lesions from normal mucosa and benign lesions in humans. *Head Neck*. 2015 Apr; 37(4):511–7. [PubMed: 24677300]
18. Mittal R, Balu M, Krasieva T, Potma EO, Elkeeb L, Zachary CB, Wilder-Smith P. Evaluation of Stimulated Raman Scattering Microscopy for Identifying Squamous Cell Carcinoma in Human Skin. *Lasers in Surgery and Medicine*. 2013; 45:496–502. [PubMed: 23996592]
19. Freudiger CW, Yang W, Holtom GR, Peyghambarian N, Xie XS, Kieu KQ. Stimulated Raman scattering microscopy with a robust fibre laser source. *Nature Photonics*. 2014; 8:153–159. [PubMed: 25313312]

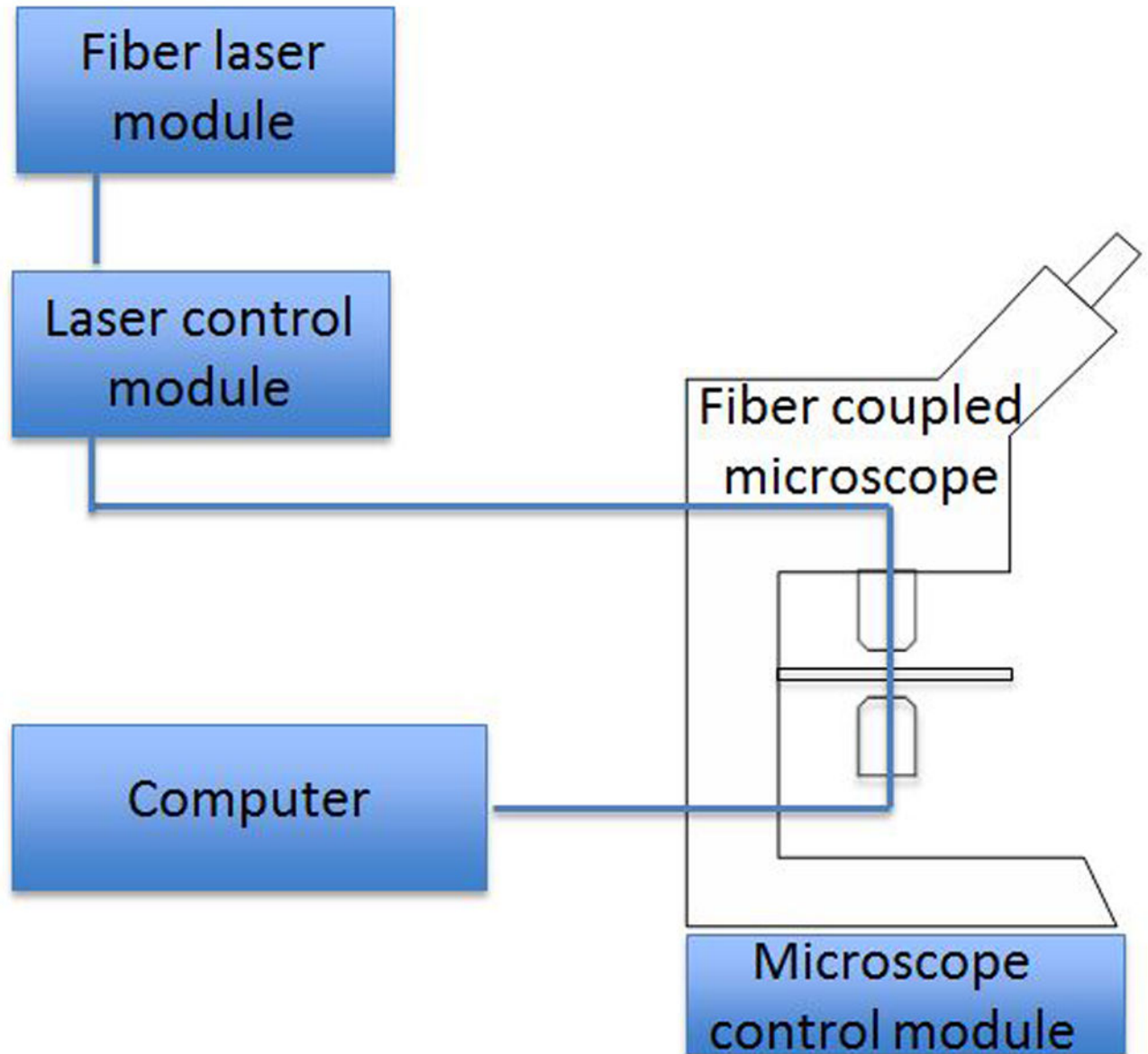


**Figure 1.**

Representative setup of CRS microscopy. Photons from the fiber laser module are tuned to specific frequencies in the laser control module and then pass through the specimen placed on the fiber coupled microscope. Intensity loss is detected and then the image displayed on a computer. Differences in Raman spectrum reflect variations in the lipid/protein ratio, which provides the contrast for the images.



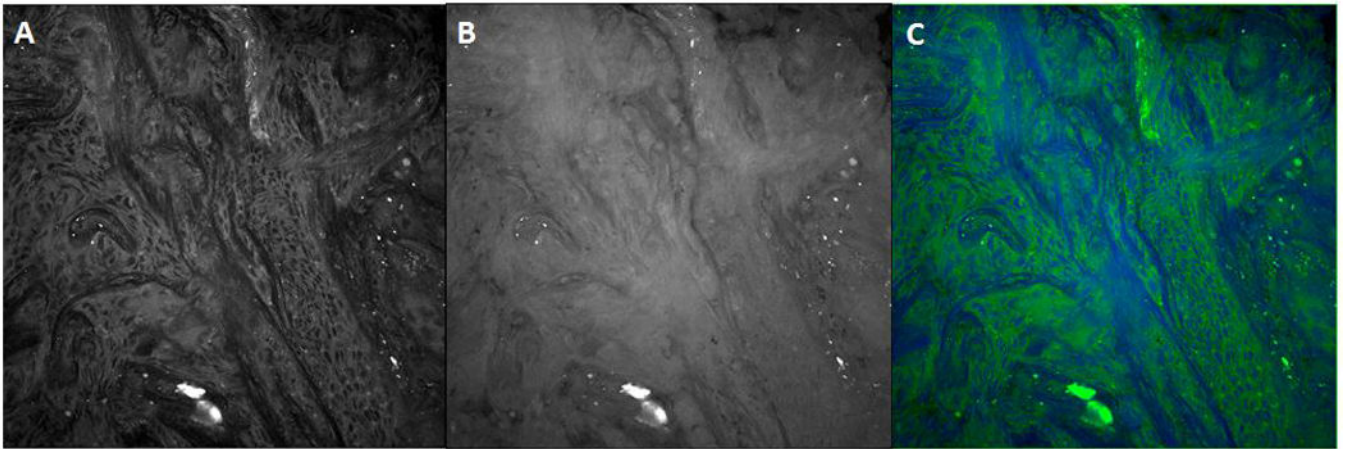


**Figure 2.** Coherent Raman scattering images of fresh squamous cell carcinoma biopsy. (A) CRS image at CH<sub>2</sub>-stretching vibration at 2845 cm<sup>-1</sup>, (B) CRS image at CH<sub>3</sub>-stretching vibration at 2940cm<sup>-1</sup>, (C) CRS image generated from A and B showing CH<sub>3</sub>-CH<sub>2</sub> difference.

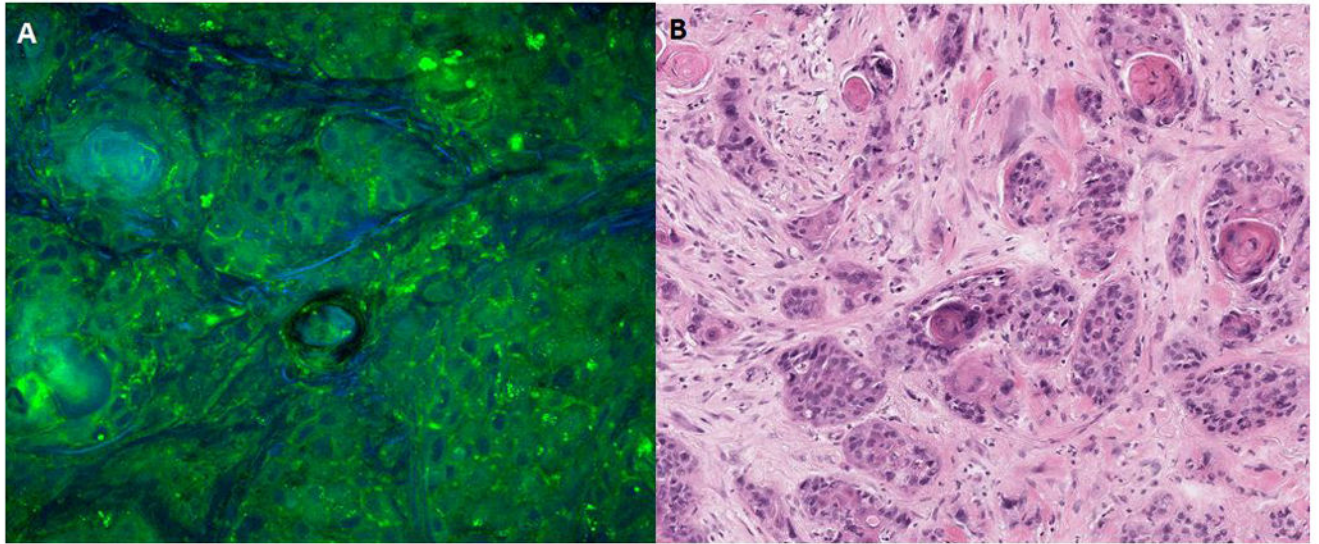


**Figure 3.** Comparison of CRS microscopy to matched H&E stained specimen. A) CRS microscopy image, demonstrating hypercellularity and atypical nuclei. B) Matched H&E stained specimen.

**Table 1**  
**Characteristics of 42 confirmed carcinoma tumor specimens**

<b>Carcinoma Type:</b>	
Squamous Cell Carcinoma	44 (96.7%)
Adenocarcinoma	1 (3.3%)
<b>Differentiation by Histopathology:</b>	
Well differentiated/low grade	4 (13.3%)
Moderately differentiated	19 (63.3%)
Moderate to poorly differentiated	2 (6.7%)
Poorly differentiated	5 (16.7%)
<b>Tissue Type:</b>	
Mucosal	25 (83.3%)
Nodal	2 (6.7%)
Cutaneous	3 (10.0%)
<b>Subsite:</b>	
Oral Cavity	14 (46.7%)
Larynx	8 (26.7%)
Oropharynx	3 (10.0%)
Unknown	1 (3.3%)
Hypopharynx	1 (3.3%)
Scalp	3 (10.0%)

**Table 2**  
**Sensitivity and specificity of CRS microscopy compared with standard H&E**

	<b>Malignant by Gold Standard H&amp;E</b>	<b>Benign by Gold Standard H&amp;E</b>
<b>Malignant by CRS Microscopy</b>	38/42	40/42
<b>Benign by CRS Microscopy</b>	4/42	2/42
	Sensitivity: 90.2%	Specificity: 95.2%

Author Manuscript

Author Manuscript

Author Manuscript

Author Manuscript